4.2 Influences on the Gas Turbine Cycle

Figure 6*b* highlights that changing from hydrogen to methane results in a shift of the equivalence ratio range in the gas turbine combustion chamber while the same shaft power output is maintained. Referring to Eqs. (1) and (2), scaling with equal heat flow rate and therewith equal shaft power lead to a change in the required fuel mass flow and a subsequent shift in the equivalence ratio:

$$\Phi_{\mathrm{CH_4}} = \Phi_{\mathrm{H_2}} \frac{\mathrm{LHV_{H_2}}}{\mathrm{LHV_{CH_4}}} \frac{\mathrm{SAR_{CH_4}}}{\mathrm{SAR_{H_2}}} .$$

Figure 6 also shows the shift to a more rich equivalence ratio range interval for methane resulting from the influence of the fuel lower heating value LHV and the impact of the stoichiometric air requirement SAR at similar heat flow rates and shaft power output. Since all relevant parameters are known (Table 2) the equivalence ratio shift can be calculated:

$$\Phi_{\mathrm{fuel}} = \frac{\dot{m}_{\mathrm{fuel}} \mathrm{SAR_{fuel}}}{\dot{m}_{\mathrm{air}}} = \frac{\dot{Q}}{\dot{m}_{\mathrm{air}}} \frac{\mathrm{SAR_{fuel}}}{\mathrm{LHV_{fuel}}} .$$

In the case of the APU, the coefficient $(\dot{Q}/\dot{m}_{\mathrm{air}})$ can be considered as nearly constant. Therefore, the equivalence ratio Φ is proportional to the ratio of the stoichiometric air requirement SAR divided by the lower heating value LHV:

$$\Phi \propto \frac{\mathrm{SAR_{fuel}}}{\mathrm{LHV_{fuel}}} .$$

The determined ratios and the equivalence ratio shift of methane and hydrogen against kerosene are compared in Table 2. The result of the equivalence ratio shift shows that the equivalence ratio of hydrogen is about 16.7% leaner compared to kerosene while methane remains in nearly identical order to kerosene, but is slightly richer.

Figure 7 shows that between methane and hydrogen, there is an offset in the EGT. The EGT of methane is higher compared to the EGT of hydrogen by about 17 K at 100% shaft power. Comparing Figs. 6 and 7, the richer fuel

Table 2 Properties of hydrogen, kerosene and methane, equivalence ratio shift relative to kerosene [16–18]

Component	$\mathrm{SAR_{fuel}}$, $\mathrm{kg_{Air}/kg_{fuel}}$	$\mathrm{LHV_{fuel}}$, MJ/kg	$\frac{\mathrm{SAR_{fuel}}}{\mathrm{LHV_{fuel}}}$	Φ-shift	Φ-shift, %
Hydrogen, (H_2)	34.3	119.95	0.2860	0.8326	−16.74
Kerosene (Jet A-1)	14.7	42.80	0.3435	1.0000	0
Methane (CH_4)	17.2	50.03	0.3438	1.0009	+0.09

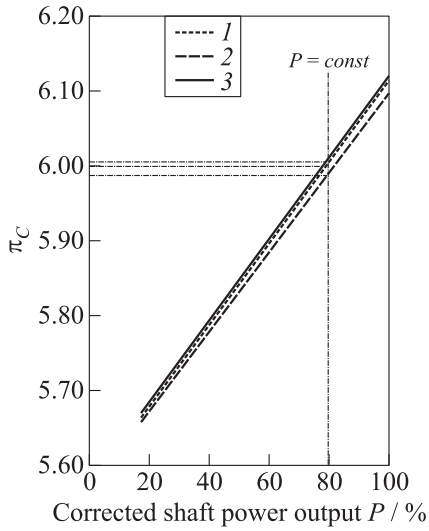

Figure 8 Compressor pressure ratio: *1* — CH_4; *2* — H_2; and *3* — kerosene

mixture at methane operation and the leaner mixture at hydrogen operation resulting from the Φ-shift lead to different combustion temperatures changing the EGT on the turbine exit and, surely, will have effects on the operational point of the gas turbine.

In Fig. 8, the compressor pressure ratio π_C is depicted vs. the corrected shaft power output P of kerosene, methane, and hydrogen. It can be observed that for a constant shaft power, the pressure ratio of the compressor changes for different fuels. In Fig. 9, the compressor characteristics are shown schematically for constant power. The APU GTCP 36-300 is a rotational speed controlled gas turbine running on constant 99% rotational speed for all ECS load conditions and on constant 101% speed in MES mode independent from the used fuel. The schematic presents that the operational point at constant power is shifted downwards along the line of operation with constant speed from kerosene over methane to hydrogen and show that the characteristics of the compressor, i. e., the compressor pressure ratio and the air mass flow through the compressor, must change. Two different effects must be considered here:

(1) when the operational point of the gas turbine changes along the line of constant speed in the compressor map, the efficiency and the performance requirements of the turbine change, too. Since the compressor pressure ratio π_C is influenced, the total efficiency η_t of the gas turbine cycle is also slightly affected, i. e., when π_C decreases, η_t decreases. Simultaneously, the air mass flow $\dot{m}_{\text{air}}$ increases and results in a shift of the specific enthalpy ratio. It can be stated that the shift in the cycle operation point is influenced mostly by the change in combustion temperature T_{4t}; and

(2) the cycle operational point is influenced by the different required fuel mass flows for kerosene, methane, and hydrogen. The turbine power is reduced with decreasing fuel mass flow $\dot{m}_{\text{fuel}}$ and must be compensated in an increase of the enthalpy Δh_T:

$$P_t \approx (\dot{m}_{\text{air}} + \dot{m}_{\text{fuel}})\, \Delta h_T \,.$$

Figure 9 shows that the shift along the operational line in the compressor map for hydrogen, methane, and kerosene is influenced by the combustion temperature T_{4t}. Each kerosene, methane, and hydrogen generates different combustion temperatures changing the operational point and the efficiency in the turbine. Generally, the influences on the efficiency of the turbine and the cycle are minor, the interaction between T_{4t} and c_{pm} $(\overline{\overline{c}}_p)$ are the dominant drivers for this phenomenon. The enthalpy in the turbine is

$$\Delta h_T \approx \overline{\overline{c}}_p T_{4t} \left(1 - \tau_t\right) .$$

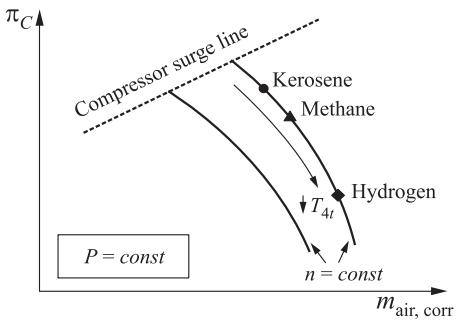

Figure 9 Schematic compressor map

Figure 10 points out the differences in the combustion temperature T_{4t}. In the figure, the difference ΔT_{4t} between methane and kerosene and the difference between hydrogen and kerosene is presented calculated by GasTurb. At constant 100% power, T_{4t} of methane is about 7 K lower as the combustion temperature of kerosene. For hydrogen compared to kerosene, the difference is even about 18 K lower matching the theory of Fig. 9. In Fig. 10*b*, the combustion temperature T_{4t} is shown in relation to the equivalence ratio. Comparing Figs. 10*a* and 10*b*, it can be observed that the differences of T_{4t} both of methane and hydrogen related to kerosene are not the same. Figure 10*a* shows the combustion temperature difference including the effect of the Φ-shift and the subsequent combustion temperature $T_{4t} = f(\Phi)$. In Fig. 10*b*, the temperature effect alone is depicted. It can be seen that at a constant equivalence ratio, hydrogen burns much hotter than methane. The Φ-shift

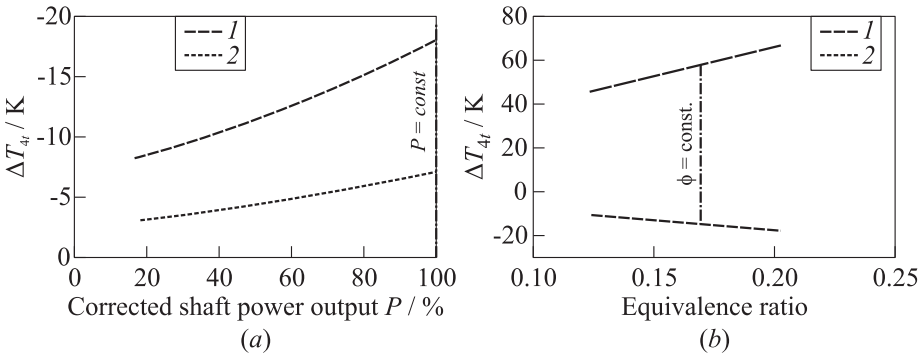

Figure 10 Combustion temperature difference related to kerosene calculated with GasTurb: *1* — methane–kerosene; and *2* — hydrogen–kerosene

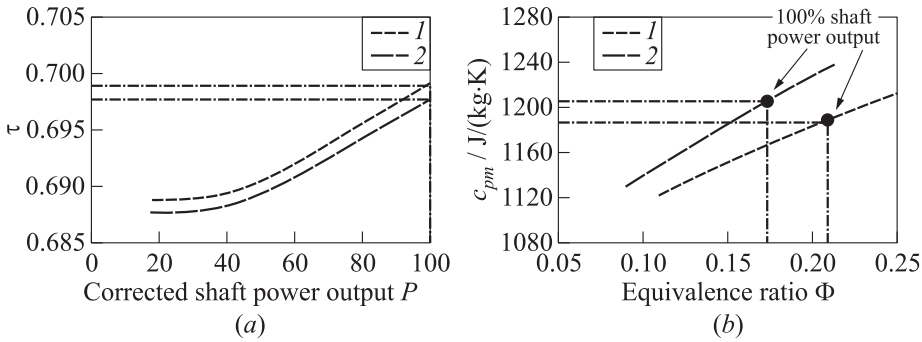

Figure 11 Turbine temperature ratio (a) and isobaric heat capacity (b): *1* — CH_4; and *2* — H_2

leads to the effect that in the gas turbine, in fact, the hydrogen burns colder than kerosene and methane confirming the theory of Fig. 8.

Regarding the T_{4t}-effect, a decrease leads to a lower turbine performance, but Fig. 10a shows that 100% shaft power are maintained. Besides, the combustion temperature, the impact of the mean isobaric heat capacity c_{pm}, and the turbine temperature ratio $\tau_t = T_{5t}/T_{4t}$ should be considered. Comparing the 100% shaft power output point in Fig. 11, the diagram shows that τ_t of hydrogen is lower than the τ_t of methane. The mean isobaric heat capacity c_{pm} is depending on the equivalence ratio at the 100% power point. For hydrogen, c_{pm} at 100% power is higher than c_{pm} of methane. For the hydrogen operation, the higher c_{pm} combined with the reduced τ_t for hydrogen both have positive effects on the turbine enthalpy maintaining turbine power for 100% shaft power output together with a reduced fuel flow.

It can be stated that for hydrogen, the impact of τ_t and c_{pm} is dominant while for methane, the T_{4t}-temperature effect is most significant.

Another effect should be also considered for τ_t. Figure 10a shows that methane and hydrogen both have a lower combustion temperature compared to kerosene at constant power. As described earlier, the power of a gas turbine could be increased by scaling the combustion temperature (turbine inlet temperature) equal to kerosene generating more power and matching the same turbine inlet conditions. But as a result of the turbine temperature ratio τ_t, it should be considered that the parts at the turbine exit are charged by higher temperatures as normal leading to life time reduction or even failure. Scaling to the same EGT T_{5t}, the effect remains the same, but the influence is different and while the parts at the turbine exit are normally charged, the area at the turbine inlet is affected by excessive heat. An increase in power of an existing gas turbine by the change of fuel with a higher heating value is possible, but sensitive considerations and modifications of the turbine cooling system should be taken into account.

The presented theoretical investigation of the gas turbine cycle supported by GasTurb shows that the change of fuel has significant impact on the gas turbine. The fuel properties influence the fuel–air mixture in the combustion chamber and lead to an equivalence ratio shift and different combustion temperatures. This affects the operational point of the gas turbine at constant power because the compressor and turbine characteristics are changed. The balance between the combustion temperature, the mean isobaric heat capacity, and the turbine temperature ratio influences turbine characteristics and also the EGT level while the turbine power remains almost constant. This has an impact on the control strategy of the gas turbine when EGT control is applied, but the benefit of possible increased gas turbine power switching from kerosene to methane and hydrogen arises.

5 CONCLUDING REMARKS

It is possible to convert a gas turbine for the use of gaseous fuels and to operate it alternatively with hydrogen and methane. For alternating dual-fuel-operation, no mechanical changes of the gas turbine are required, only slight modifications of the start-up-controller software are necessary regarding ignition and initial acceleration. In a future scope of work, the gas turbine main engine controller can be optimized by improving the on-speed-governor for the dual-fuel operation with hydrogen and methane implementing adaptable control parameters when switching between fuels.

The theoretical investigation of the thermodynamic cycle shows that the change of fuel has a significant impact on the gas turbine operation point. An equivalence ratio shift occurs and affects the combustion temperature at constant gas turbine power changing the characteristics of compressor and turbine.

Additionally, hydrogen gives the opportunity to increase the power output of an existing gas turbine at equal EGTs like kerosene or methane, but the influences of different behavior in the turbine temperature ratio should be considered to avoid overheating of turbine parts. Another interesting aspect is that when changing a gas turbine from kerosene or methane to hydrogen, hydrogen burns at lower temperatures while the same gas turbine power output level is preserved. This leads to the opportunity to increase the turbine section hot parts life time, because the prevailing temperatures at the turbine inlet are reduced.

REFERENCES

1. Lieuwen, T., V. Yang, and R. Yetter, eds. 2009. *Synthesis gas combustion: Fundamentals and applications*. Boca Raton – London – New York: CRC Press. 400 p.
2. Suttrop, F., and R. Dorneiski. 1991. Low NOx-potential of hydrogen-fuelled gas turbine engines. *1st Conference (International) on Combustion Technologies for a Clean Environment*. Vilamoura, Portugal.

3. Dahl, G., and F. Suttrop. 1998. Engine control and low-NOx combustion for hydrogen fuelled aircraft gas turbines. *Int. J. Hydrogen Energy* 23:695–704.
4. Funke, H. H.-W., S. Börner, P. Hendrick, and E. Recker. 2011. Modification and testing of an engine and fuel control system for a hydrogen fuelled gas turbine. *Progress in propulsion physics*. Eds. L. DeLuca, C. Bonnal, O. Haidn, and S. Frolov. EUCASS advances in aerospace sciences book ser. 2:475–486.
5. Funke, H. H.-W., S. Börner, P. Hendrick, and E. Recker. 2010. Control system modifications for a hydrogen fuelled gas-turbine. *13th Symposium (International) on Transport Phenomena and Dynamics of Rotating Machinery (ISROMAC13)*.
6. Funke, H. H.-W., S. Börner, P. Hendrick, E. Recker, and R. Elsing. 2011. Development and integration of a scalable low NOx combustion chamber for a hydrogen fuelled aero gas turbine. *4th European Conference for Aeronautics and Space Sciences (EUCASS)*. St. Petersburg.
7. Börner, S., H. H.-W. Funke, F. Falk, and P. Hendrick. 2011. Control system modifications and their effects on the operation of a hydrogen-fueled Auxiliary Power Unit. *20th Symposium (International) on Air Breathing Engines (ISABE 2011)*.
8. Westfalen AG. 2015. Hydrogen — safety data sheet.
9. Westfalen AG. 2015. Methane — safety data sheet.
10. Chiesa, P., G. Lozza, and L. Mazzocchi. 2005. Using hydrogen as gas turbine fuel. *Trans. ASME J. Eng. Gas Turbines Power* 127(1):73–81.
11. Verstraete, D., P. Hendrick, P. Pilidis, and K. Ramsden. 2005. Hydrogen as an (aero) gas turbine fuel. *17th Symposium (International) on Air Breathing Engines (ISABE 2005)*.
12. Kurzke, J. 2007. GasTurb: Design and off-design performance of gas turbines. Software Manual. http://www.gasturb.de/manual.html (accessed October 30, 2015).
13. Kurzke, J. 2005. How to create a performance model of a gas turbine from a limited amount of information. *ASME Turbo Expo 2005: Power for Land, Sea and Air Proceedings*. American Society of Machanical Engineers. 145–153.
14. Kurzke, J. 1996. How to get component maps for aircraft gas turbine performance calculations. *International Gas Turbine and Aeroengine Congress & Exhibition of the American Society of Mechanical Engineering Proceedings*. American Society of Machanical Engineers. V005T16A001–V005T16A001.
15. Kurzke, J. 2003. Model based gas turbine parameter corrections. *ASME Turbo Expo 2003 collocated with the 2003 Joint Power Generation Conference (International) Proceedings*. American Society of Machanical Engineers. 91–99.
16. Deutsches Institut für Normung e.V. 1997. Berechnung von Brennwert, Heizwert, Dichte, relativer Dichte und Wobbeindex von Gasen und Gasgemischen. *DIN* 51857:1997-03.
17. Exxon Mobil Aviation. 2008. World jet fuel specifications with avgas supplement. Machelon: ExxonMobil Aviation. Available at: http://www.exxonmobil.com/AviationGlobal/Files/WorldJetFuelSpec2008_1.pdf. (accessed October 30, 2015).
18. Esch, Th. 2011. *Verbrennungstechnik — combustion technology: Textbook*. 8th ed. Aachen: Department of Aerospace Engineering, Aachen University of Applied Sciences. Unpubl.